



PEFORMANCE OF EXISTING REINFORCED CONCRETE COLUMNS UNDER SHEAR & AXIAL LOADING

MSc Eng.Damawand M.Karim

1 Introduction

1.1 BACKGROUND

Existing reinforced concrete structures designed before the introduction of modern seismic code in the early 1970's are vulnerable to damage and collapse during an earthquake. Prior to the FEMA124 establishment of performance-based earthquake design specifications, reinforced concrete structures utilized in bridges and buildings were designed in accordance with AASHTO code which only required that reinforced concrete structures sustain a single hazard or maximum loading event. Often, these requirements resulted in the design of reinforced concrete columns with minimal transverse reinforcement (i.e. column confinement), highly spaced stirrups and/or low longitudinal reinforcement ratios. Thus, such structures inevitably experience significant column buckling, undergo excessive shear drift and degradation of shear and axial load capacity which pose a substantial danger to building occupants or bridge pedestrians supported by such columns.

Thus, it is vital that reinforced concrete structures, especially life-safety structures not designed in accordance to modern performance-based earthquake code, be retrofitted to sustain seismic loading. It is often more economically feasible to retrofit vulnerable existing reinforced concrete structures than to completely replace them. However, to properly strengthen these vulnerable reinforced concrete structures against complex seismic loading patterns, it is imperative to first understand the progression of damage and mechanisms causing collapse in reinforced concrete columns and frames.

1.2 PREVIOUS RESEARCH

Experimental research and post-earthquake investigations conducted in the past have produced numerous findings about the behavior of reinforced concrete columns under gravity and seismic load. Elwood and Moehle (2003) give a brief overview of experimental results based on various shear and axial loading tests performed on reinforced concrete columns and/or frames which form the foundation of this research. From the results, it was suggested that a loss of axial load capacity in a reinforced concrete column does not always immediately occur after a loss of shear capacity (Elwood and Moehle, 2003; Sezen, 2002). Also, it was observed that the lateral displacement or drift of a reinforced concrete column at axial failure is dependent upon and directly proportional to the spacing of transverse reinforcement and the axial stress developed within the column.

Elwood and Moehle state that from many pseudo-static tests that examined axial capacity in shear-damaged columns (Yoshimura and Yamanaka, 2000; Nakamura and Yoshimura, 2002; Tasai, 1999; Tasai, 2000; Kato and Ohnishi, 2002; Kabeyasawa et al., 2002), axial failure occurred when the columns lost all shear capacity. Further, it was noted that the lateral drift experienced by the column at axial failure was dependent upon and inversely proportional to the amount of axial load exerted on the column. From the research findings of Tasai (2000), Elwood

and Moehle note that the total lateral drift experienced by a column was dependent upon and inversely proportional to the column's residual axial capacity. Lastly, from the tests conducted by Minowa, et al. (1995), Elwood and Moehle stated that reinforced concrete columns with closer transverse reinforcement spacing sustained gravity loads at larger lateral displacements after shear failure than those columns having wider stirrup spacing.

1.3 OBJECTIVES AND SCOPE

Since the process by which shear failure degrades the residual axial capacity of a column is not well understood in columns designed prior to the introduction of modern seismic code, it is my objective to conduct such research. Test results that have been obtained for reinforced concrete columns suggest certain relationships between structural parameters; such relationships have been used to develop predictive hysteretic response and drift models and subsequently, analytical models by which to use in future verification studies of large scale structural testing. First, however, the ability of the *OpenSees* analytical model to accurately predict the interaction between the shear and axial capacity of the column must first be established; a verification study to predict the hysteretic response of a shear-critical reinforced concrete column under lateral and gravity load will be the focus of this study.

This study is limited to reinforced concrete columns that can be characterized by a shear - failure mode. Further, all hysteretic response and drift analysis is carried out assuming that the reinforced concrete column specimen behaves as a two-dimensional column under a cyclic, unidirectional lateral loading and constant gravity load; it is also assumed that throughout the experimental test program, the column base behaves elastically.

1.4 ORGANIZATION

This report is organized in the following manner: presentation of predictive capacity models; fabrication of column test specimens and experimental setup; experimental test program; presentation of test results; validation study between test results and analytical model predictions.

2 Linear-Elastic Response of RC Column

2.1 CAPACITY MODELS

A shear-critical reinforced concrete column is a column that fails in shear prior to yielding in flexure; thus, a shear-critical column will tend to exhibit a brittle mode of failure rather than the preferred ductile model of failure. Since such a column can fail suddenly when the shear load demand on the column exceeds its shear capacity, the design of a shear-critical reinforced concrete column is governed by the shear loading that must be sustained by the column.

In order to assess the maximum shear loading that will be applied to the column, one must take into account the moment at the base-column joint induced by the lateral loading when designing the column. Further, since reinforced concrete columns primarily act as supports to other structures, it is critical that such columns be designed to sustain gravity loads, in addition to seismic-induced lateral loading.

2.1.1 Axial Load

The axial load capacity of a reinforced concrete column depends on the axial load capacity of the longitudinal reinforcement, as well as the axial capacity carried by the concrete. According to MacGregor (1998) and ACI Code, the following equation is used to assess the maximum axial load capacity, P_N of a reinforced concrete column:

$$P_N = 0.85f_C'(A_G - A_{SL}) + f_{YL}A_{SL} \quad (2.1)$$

where the first term, $0.85f_C'(A_G - A_{SL})$ represents the axial capacity carried by the concrete and the second term, $f_{YL}A_{SL}$ represents the axial capacity carried by the longitudinal reinforcement. f_C' is the specified 28-day compressive strength of concrete (ksi), f_{YL} is the yield strength of the longitudinal reinforcement (ksi), A_G is the gross area of the column cross section and A_{SL} is the area of the longitudinal reinforcement. The maximum axial load capacity in a column is achieved when no flexural moment is induced in a column.

2.1.2 Flexure

The moment or flexural capacity of a reinforced concrete column depends on the cross section of the column. Given the cross section of the shear-critical column considered in this project, the maximum moment capacity of the column can be assessed by summing the internal forces from the longitudinal reinforcement and concrete about the centroid of the column.

The following equation is derived from Figure 2.1 and is used to evaluate the maximum moment capacity of a reinforced concrete column, M_N :

$$M_N = T_{S3}[(h/2) - d_{S3}] - C_C[(h/2) - (a/2)] + T_{S1}[d_{S1} - (h/2)] \quad (2.2)$$

where T_{Si} is the internal tensile force provided by the longitudinal reinforcement i , C_C is the internal compressive force of the concrete, h is cross section depth, a is depth of stress block, and d_{Si} is the distance from extreme compression fiber to reinforcement layer i . The maximum moment capacity of a column can only be reached if there are no axial loads applied to the column.

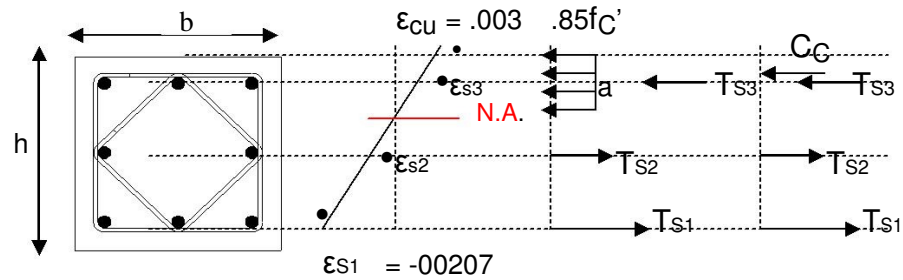


Figure 2.1: Cross section analysis used to compute the moment capacity of a reinforced concrete column.

2.1.3 Shear

The total shear capacity of a reinforced concrete column depends on the shear capacity of the concrete, V_C and the shear capacity carried by the transverse reinforcement, V_{ST} . According to MacGregor (1998) and ACI Code, the following equation is used to assess the maximum shear capacity, V_N of a reinforced concrete column subjected to combined shear, moment and axial compression loading:

$$V_N = V_C + V_{ST} = 2[1 + (P/[2000A_G])] \sqrt{f_C} b_w d + (A_{ST} f_{YT} d) / s \quad (2.3)$$

where P is the applied axial load, b_w is the width of the column cross section, s is the transverse reinforcement spacing, d is the distance from extreme compression fiber to farthest tensile reinforcement, A_{ST} is the area of the transverse reinforcement, f_{YT} is the yield strength of the transverse reinforcement.

2.2 INTERACTION DIAGRAM

The load capacity of a reinforced concrete column subjected to both flexural and axial loading can be assessed from an interaction diagram; such a diagram shows the relationship between the axial load capacity and moment capacity of a reinforced concrete column prior to yielding of the longitudinal reinforcement. If the moment and axial load capacity of a reinforced concrete column is evaluated for different tensile yield strains, an interaction diagram can be plotted. Figure 2.1 shows an interaction diagram for the column cross sections considered in this project.

2.3 YIELD DISPLACEMENT

The lateral displacement under which the longitudinal reinforcement in the column first yields can be evaluated as a sum of three deformation components. The three deformation components that contribute to the overall yield displacement of the column are displacement due to flexure, bar (bond) slip and shear.

$$\Delta_{Y \text{ calc}} = \Delta_{FL} + \Delta_{SL} + \Delta_{SH} \quad (2.4)$$

2.3.1 Flexure Deformation

For a column that is fixed against rotation at both ends, flexural deformation results when a moment load is induced in the column and a lateral displacement occurs at the ends since there are no end restraints against horizontal displacement. Figure 2.2 exhibits this concept.

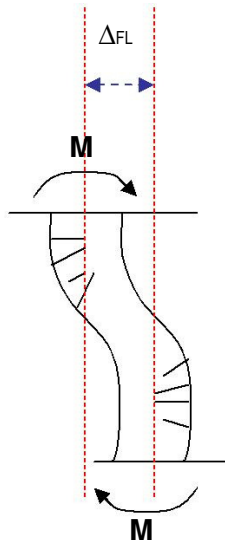


Figure 2.2: Flexural deformation in a column.

The following empirical equation, presented in Elwood and Moehle (2003), is used to estimate the lateral displacement due to flexure before yielding of the longitudinal reinforcement occurs:

$$\Delta_{FL} = L^2 \Phi_Y / 6 \quad (2.5)$$

where L is the column length and Φ_Y is the column curvature at yielding of the longitudinal reinforcement.

2.3.2 Bar (Bond) Slip

For a reinforced concrete column subjected to lateral load, slip of the longitudinal reinforcement within the anchor block of the column can occur; an elongation of the longitudinal reinforcement at the column-base joint results which then produces an additional lateral displacement in addition to the those caused by flexure. Figure 2.3 exhibits this concept.

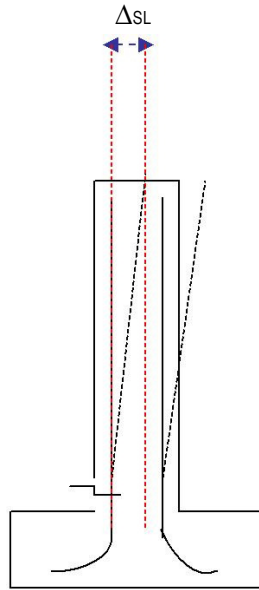


Figure 2.3: Bar (bond) slip in a column.

The following equation, derived in Elwood and Moehle (2003), is used to estimate the lateral displacement due to bar or bond slip before yielding of the longitudinal reinforcement occurs:

$$\Delta_{SL} = L d_B f_{YL} \Phi_Y / 8u \quad (2.6)$$

where d_B is the diameter of the longitudinal reinforcement and $u = 6\sqrt{f_C}$ (psi unit) is the bond stress between the longitudinal reinforcement and the column footing.

2.3.3 Shear

For a column that is fixed against rotation at both ends, shear deformation results when lateral loading produces shear stresses at the column ends resulting in displacement. This concept is exhibited in Figure 2.4.

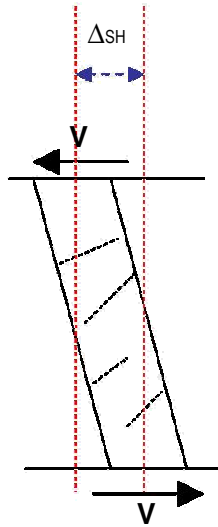


Figure 2.4: Shear deformation in a column.

The following empirical equation, presented in Elwood and Moehle (2003), is used to estimate the lateral displacement due to shear before yielding of the longitudinal reinforcement occurs:

$$\Delta_{SH} = 2M_Y / GA_V \quad (2.7)$$

where M_Y is the column moment at yielding of the longitudinal reinforcement, G is the shear modulus assuming the column is homogeneous in material, $A_V = 5/6 A_G$ is the shear area of the column cross section.

3 Inelastic Response of RC Column

3.1 INTRODUCTION

After the longitudinal reinforcement in a shear-critical reinforced concrete column yields, the column continues to undergo further lateral drift (i.e. plastic deformation) until the shear demand on the column exceeds its shear capacity. When the column's shear capacity is exceeded, shear failure and a loss of axial load capacity occurs.

3.2 MOMENT CURVATURE RESPONSE

While an interaction diagram is useful to assess the interaction between a reinforced concrete column's axial and moment capacity prior to yielding of the longitudinal reinforcement, another model is required to evaluate the degradation of shear capacity and subsequent loss of axial load capacity in a column, after yielding of the longitudinal reinforcement and at increasing lateral drifts. A moment curvature analysis relates the moment and curvature of a reinforced concrete

column at drifts beyond yield and thus, is used to evaluate the plastic response of a reinforced concrete column under shear and axial loading.

Since the shear-critical reinforced concrete column specimens tested in this project are to be loaded beyond shear failure, a moment curvature analysis will be more useful in this project for the analysis of the column's drift response to shear and axial loading. The analytical finite element program *OpenSees* is initially used to conduct a cross section analysis of the column specimens considered and a moment curvature response is then developed for the columns; utilizing Equations 2.4 to 2.7, the displacement at which yielding of the longitudinal reinforcement, shear failure and axial load failure occurs is then computed.

4 Shear Drift Capacity Model

4.1 INTRODUCTION

Conventional force -based drift capacity models (i.e. shear strength model) used to model the plastic behavior of shear -loaded columns are usually not appropriate when used to evaluate the drift of columns at shear failure since the force demand on a column remains constant after yielding while the displacement experienced by the column does not. As stipulated by Elwood and Moehle (2003), a displacement -based model is more useful when computing drift at shear failure. Thus, Elwood and Moehle (2003) develop an empirical shear drift capacity model that represents the shear strength degradation of a shear-critical reinforced concrete column and is also valid to access lateral displacement or drift beyond shear failure.

4.2 EXPERIMENTAL DATABASE

The empirical shear drift capacity model proposed by Elwood and Moehle (2003) is based on data from 40 prior (unidirectional loaded) tests conducted on shear-critical reinforced concrete columns and thus, the model is only valid to assess column drift behavior beyond yielding for those shear-critical columns with properties within those specified in the database. The shear-critical column specimens considered in this project were checked against the properties of those tested columns in the database and are found to be similar. Thus, utilizing the empirical drift capacity model to assess drift at shear failure of my specimens is valid.

4.3 DISPLACEMENT-BASED EMPIRICAL DRIFT CAPACITY MODEL

The empirical drift capacity model developed by Elwood and Moehle (2003) for reinforced concrete columns differs from earlier models since it is based, not on the performance of columns designed in accordance to modern seismic code, but rather, on older columns which fail in shear prior to the occurrence of flexural yielding (due to limited transverse reinforcement). Since this research focuses on the interaction between shear and axial capacity loss in shear-critical columns, the drift capacity model was utilized into this study.

4.3.1 Drift Ratio at Shear Failure

To quantify the lateral deformation occurring in a shear-critical reinforced concrete column subjected to shear and axial loading, a drift ratio is employed to illustrate column deformation in relation to the column's length. The following empirical equation developed by Elwood and Moehle (2003) is used to estimate the drift ratio at shear failure, (Δ_{SH} / L) of a shear-critical reinforced concrete column subjected to axial loading:

$$(\Delta_{SH} / L) = (3/100) + 4\rho'' - (1/500)(u/\sqrt{f_C'}) - [P/(40A_G f_C')] \geq (1/100) \quad (4.1)$$

where $\rho'' = (A_{ST} / bs)$ is the transverse reinforcement ratio, b is the column cross section width, s is the stirrup or transverse reinforcement spacing, $u = (V_Y / bd)$ is the maximum shear stress and d is the depth to the farthest tensile reinforcement.

5 Axial Capacity Model

5.1 INTRODUCTION

Though a reinforced concrete structure may lose much of its shear strength after the occurrence of shear failure, it is important that an engineer be able to determine the column's ability to sustain gravity loads in the event of shear failure. Since total structural collapse in a reinforced concrete column is defined by axial load failure, an axial capacity model that is able to quantify the residual axial load capacity that a column possesses is required in order to establish whether the column is able to sustain gravity loads after shear failure.

5.2 CLASSICAL SHEAR-FRICTION MODEL

Based on the tests conducted by Lynn (2001) and Sezen (2002) on shear-critical reinforced concrete columns up to the point of axial failure, Elwood and Moehle (2003) develop an axial capacity model that allows one to assess the residual axial load capacity of a shear-critical reinforced concrete column after shear failure; this axial capacity model was developed with the assumption that load distribution across a column's shear failure plane occurs through the mechanism of shear friction forces.

5.2.1 Shear Failure Plane

After the occurrence of shear failure in a column, an inclined shear failure crack results as can be seen from the plane inclined at an angle, θ in Figure 5.1 that developed in a column tested by Elwood and Moehle (2003).

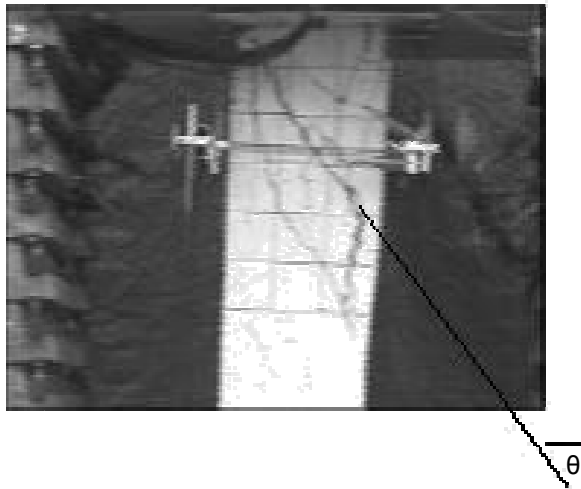


Figure 5.1: Shear failure plane in a reinforced concrete column after shear failure.

According to Elwood and Moehle (2003), once shear failure occurs in a shear -critical reinforced concrete column, gravity loads supported by the shear-damaged column must be transferred across the shear failure plane that develops if total structural collapse is to be prevented. This transfer of gravity load across the shear failure plane occurs via *shear friction forces* which arise from the internal forces of the longitudinal and transverse reinforcement.

5.2.2 Residual Axial Load Capacity

When shear failure occurs in a reinforced concrete column, gravity loads are supported by shear friction forces developed within the column and thus, the column continues to possess some axial capacity after shear failure. Figure 5.2 shows the vertical and horizontal internal forces of the longitudinal reinforcements and horizontal forces of the transverse reinforcement which produce the shear friction forces, as well as the applied shear, V and axial load, P on the column. The inclined shear failure surface is assumed to occur at a critical angle, θ which is representative of the inclined crack resulting from shear damage in the column.

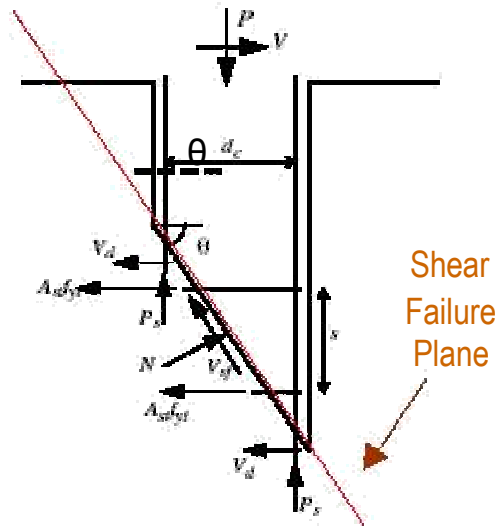


Figure 5.2: Free Body Diagram of column after shear failure.

From equilibrium of the internal and applied forces in Figure 5.2, Elwood and Moehle (2003) derived the axial load capacity of a shear-damaged column. The following equation represents the residual axial load capacity of a shear-critical, reinforced concrete column after shear failure:

$$P_R = \tan\theta[(A_{ST}F_{YT}d_C) / s][(\cos\theta - \mu_F \sin\theta) / (\sin\theta - \mu_F \cos\theta)] \quad (5.1)$$

where θ is the critical crack angle, d_C is the horizontal distance between the longitudinal reinforcement, μ_F is the effective coefficient of friction and s is the stirrup or transverse reinforcement spacing. In this report, the critical crack angle, θ is assumed to be 65° .

In the case where the effective friction coefficient and/or critical crack angle is not known prior to testing, the residual axial load capacity of a shear-critical, reinforced concrete column can reasonably be estimated as ten percent of the undamaged axial load capacity of the column, P_N as computed from Equation 2.1. This method of computing the residual axial capacity of the column specimens is used in this report to approximate the axial load that will be applied in the experimental test program discussed in Chapter 6.

When the axial load demand on the column exceeds the axial capacity provided by shear friction forces, axial load failure of the column results. Axial load failure signifies total collapse of the structure and is assumed to occur when the column has zero or negligible shear strength.

5.3 DRIFT RATIO AT AXIAL LOAD FAILURE

The maximum capacity drift model developed by Elwood and Moehle (2003) was based on the results achieved by Lynn and Sezen (2002) and is used to assess the lateral drift of a shear-critical reinforced concrete column at axial failure. The maximum capacity drift model depends only on the capacity of shear friction forces and not the longitudinal bar capacity of the column

since the shear friction capacity far exceeds that of the longitudinal reinforcement, at low lateral drifts. While the total capacity drift model, which incorporates drift capacity due to shear friction and longitudinal reinforcement, accurately predicts the drift at axial load failure that occurred in the specimens tested by Lynn and Sezen (2002), Elwood and Moehle recommend using the maximum capacity drift model to assess column drift at axial failure.

Based on the maximum capacity drift model, the following equation derived by Elwood and Moehle (2003) predicts the lateral drift taking place in a shear-critical reinforced concrete column at the onset of axial load failure:

$$(\Delta_{AX} / L) = [(4/100)(1 + \tan^2 \theta)] / [\tan \theta + P(s / [A_{ST} F_{YT} d_C \tan \theta])] \quad (5.2)$$

6 Design of Quasi-Static Test

6.1 INTRODUCTION

A quasi-static test was designed to observe the process of damage progression, shear degradation and axial load failure in a shear-critical reinforced concrete column subjected to dynamic shear and constant axial loading. This chapter provides an overview of the design, construction and testing of the reinforced concrete frame specimens.

6.2 RC COLUMN SPECIMEN

Two reinforced concrete column test specimens were designed by UC Berkeley graduate student, Yoon Bong Shin to exhibit the hysteretic behavior representative of existing, shear-critical reinforced concrete columns under simulated gravity and seismic load. The geometric design of the test specimens was chosen to be representative of a typical, existing shear-critical reinforced concrete column at one-third scale. This column design as well as the selection of reinforcement is shown in Figure 6.2.

6.2.1 Prototype and Design Requirements

Two test specimens were constructed and tested. Each column specimen was designed at one-third scale and representative of a typical shear-critical reinforced concrete column. A static axial/gravity load would be applied to each specimen, a load that is determined based on the residual axial capacity of the column specimen, P_R which was taken, as previously discussed in Section 5.2.2, to be ten percent of the undamaged axial load capacity, P_N of the reinforced concrete column. Based on the cross section of the reinforced concrete column specimens, the undamaged axial load capacity of the specimens was computed to be 240.97 kips; thus, the residual axial capacity of a shear damaged column specimen was estimated as ten percent of the total column capacity, or 24.1 kips. To ensure the occurrence of axial failure in both specimens during testing, a 30 kip static gravity load would be subjected onto the columns.

In addition to gravity load, a cyclic, unidirectional shear load of approximately 8 kips, calculated as the shear load capacity of the column [Equation 2.3] and used to simulate simple seismic

loading, is also to be applied. Gravity and shear loading, as they will be applied to each column specimen, is shown in Figure 6.1b.

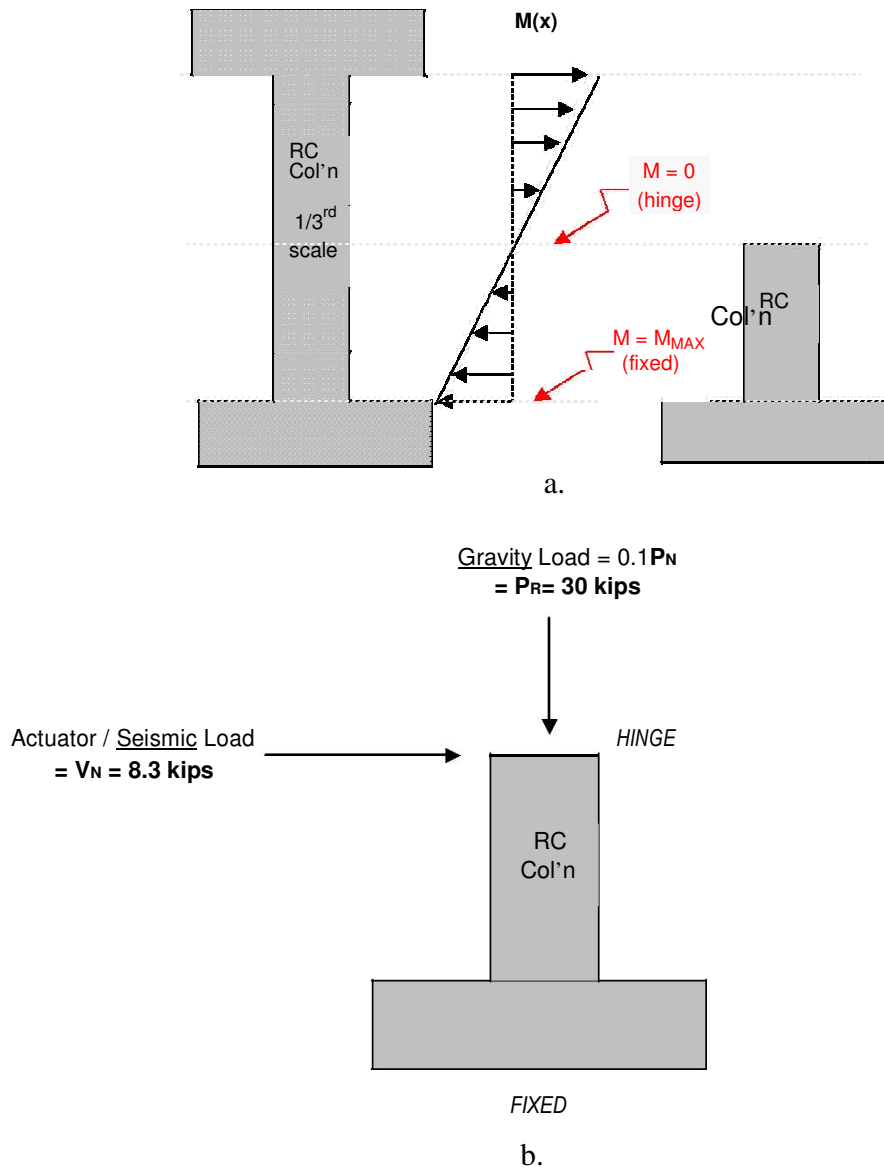


Figure 6.1: Simplified model of reinforced concrete test specimen.

a. Idealized cantilever model b. Applied loads on model

As shown in Figure 6.1a., to further simplify column analysis and fabrication in this project, the reinforced concrete column design would be idealized as a cantilever column fixed at one end and free on the opposite end; this simplification is valid for the representation of actual full column prototypes with no moment resistance at column center and maximum moment resistance at the fixed ends when it is subjected to end shear forces.

6.2.2 Geometry and Reinforcement

Each column specimen was designed and fabricated with a transverse reinforcement or tie spacing of 4 inches and a column height of 29 inches. Thus, the full-scale column prototype would have a 12 inch tie spacing for the entire column length of 87 inches making the column extremely vulnerable to shear failure, and subsequent axial load failure during the test program due to the minimal transverse reinforcement and wide tie spacing in the column.

The base of the column specimen, however, was not designed to be representative of existing reinforced concrete columns; rather, the column base was over-reinforced in design to ensure it would remain elastic throughout the testing of the specimens ensuring that shear damage and axial load failure would occur above the column-base joint.

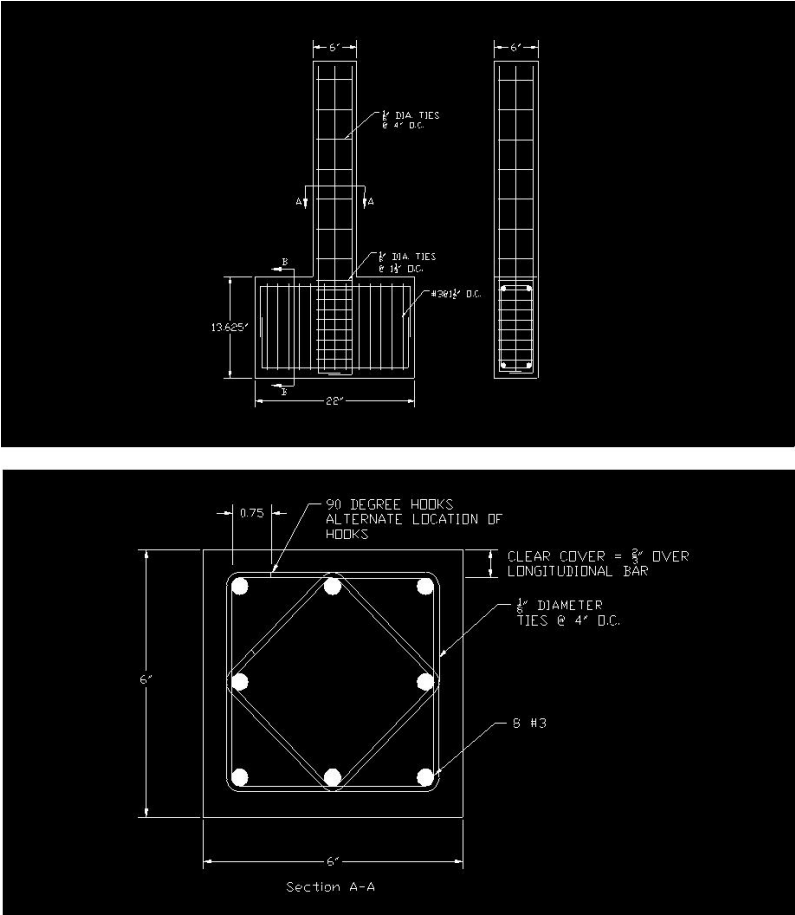


Figure 6.2: Reinforced concrete test specimen.

6.2.3 Fabrication

The test specimens were cast in a flat, horizontal position using forms fabricated previously. The column forms were constructed from marine-grade plywood and the specimens were cast at a site adjacent to the shake table lab. Steel reinforcement cages were then built using Grade 60 steel for all column reinforcement, #3 rebar for the longitudinal reinforcement, one-eighth inch diameter steel ties for the transverse reinforcement, #5 bent rebar [at 90 degree curvature] for the column base reinforcement and tie wires to hold the steel cage assembly together. Exact column reinforcement specifications are given in Figure 6.2 and the fabricated steel reinforcement cages used in the column specimens are shown in Figure 6.3.

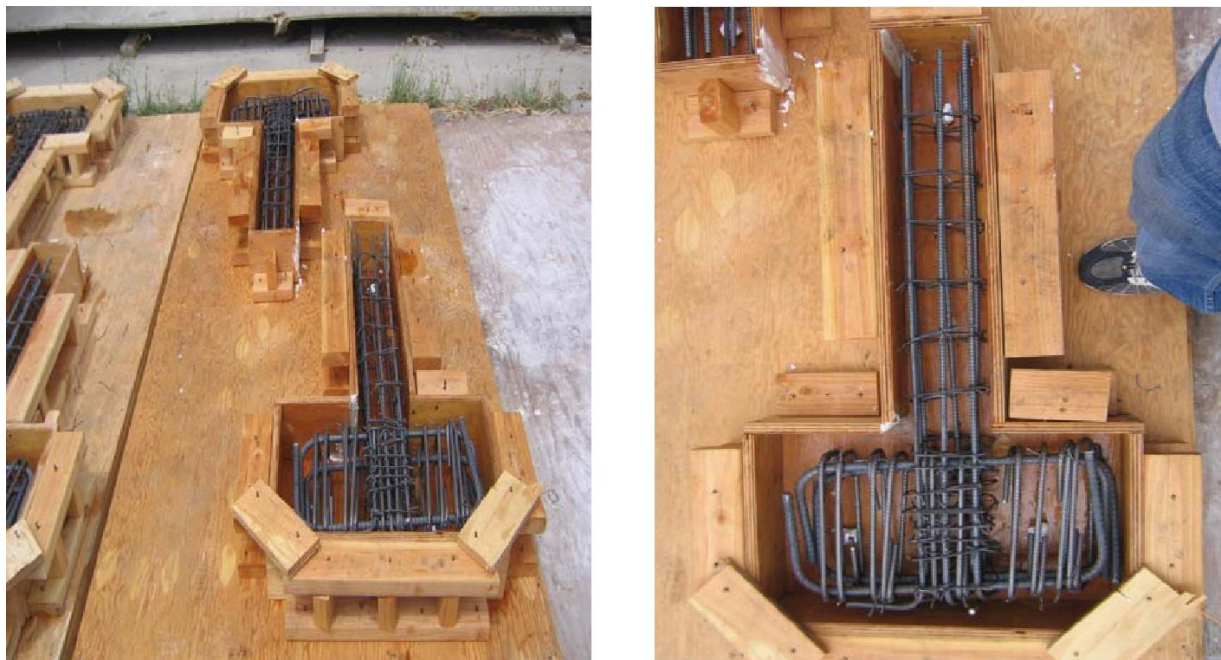


Figure 6.3: Forms and steel reinforcement cages of test specimens.

Normal -weight aggregate, high early strength concrete, with a 7-day early compressive strength of 3 ksi and an ultimate compressive strength of 6 ksi was used to cast the column specimens in one lift, as shown in Figure 6.4. Specimens were wet-cured for 22 days and then stored indoors until testing.



Figure 6.4: Casting of test specimens.

Concrete cylinders were also simultaneously fabricated, cured and stored alongside the concrete specimens for use in a crushing test. However, due to time constraints and budget considerations, the concrete cylinders were not tested for their compressive strength; thus, utilizing a concrete cure curve and based on the age at testing [specimen 1 age - 49 days, specimen 2 age - 51 days] as well as the concrete mix composition, it was estimated that the column specimens reached their ultimate compressive strength of 6 ksi by the testing date; thus, a concrete compressive strength value of 6 ksi was used in the analysis of this report.

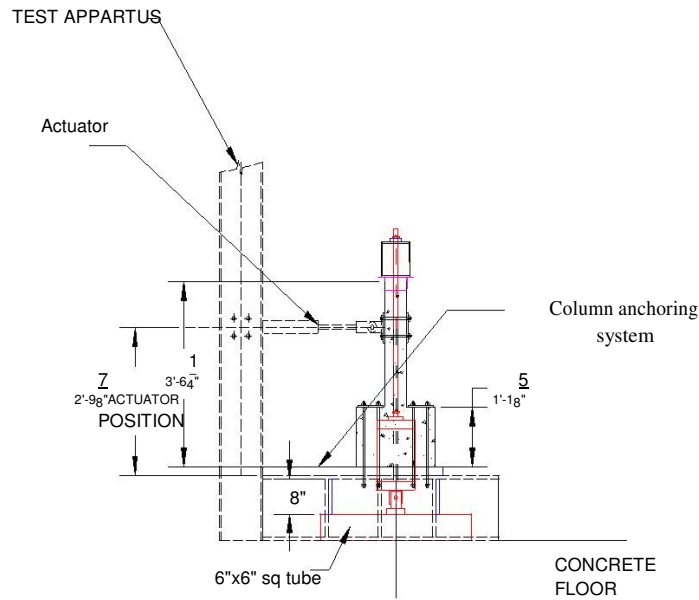
Initially, a 3 ksi compressive concrete strength was desired in order to maintain consistency with full-scale tests conducted previously on shear-critical reinforced concrete columns; however, a column compressive strength of 6 ksi would be unavoidable at the time of testing; thus, a larger shear and axial loading was computed based on the higher compressive strength such that the specimen hysteretic response curves would be comparable to that of full-scale, shear-critical reinforced concrete columns subjected to similar loading.

6.3 EXPERIMENTAL SETUP

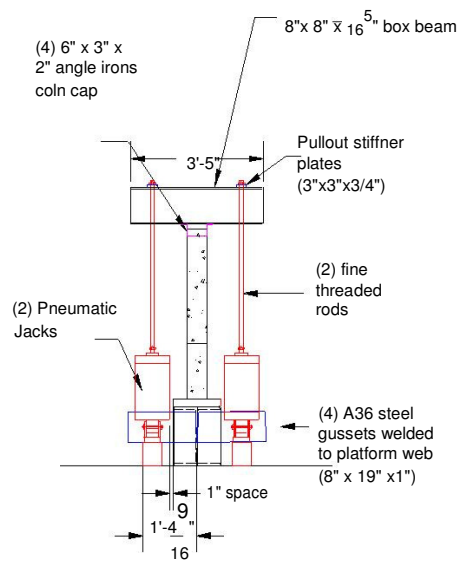
6.3.1 Design

An existing experimental setup, consisting of an actuator attached to a reaction wall and ideal for the testing of small-scale column structures was to be utilized in this study to provide a cyclic shear load on the column test specimens. However, there existed no means to subject the test specimens to a static axial load concurrently with the cyclic shear loading. Thus, after several revisions, an experimental setup was designed that would allow the test specimens to undergo bi-directional loading which simulate the gravity and unidirectional seismic loading experienced by

an actual column; Figure 6.5 shows the details of the experimental setup used in this project; the fabrication and functionality of the setup will be discussed in the following section.



FRONT VIEW



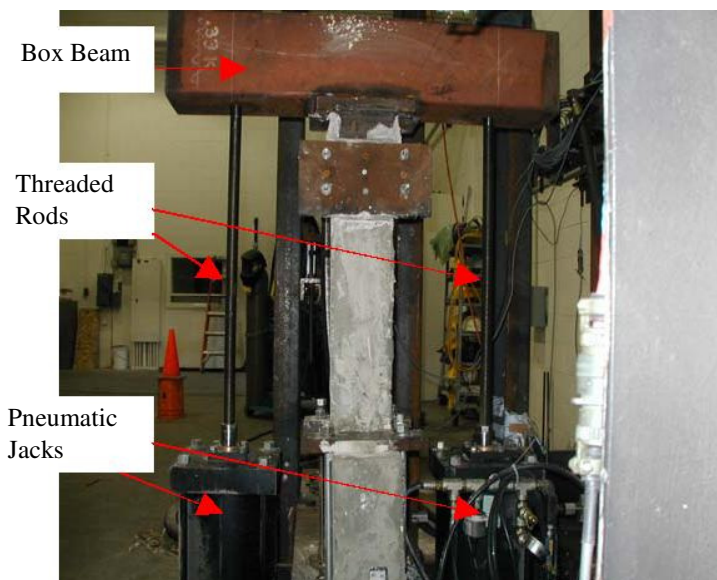
SIDE VIEW

Figure 6.5: Experimental setup design for quasi-static tests on specimens.

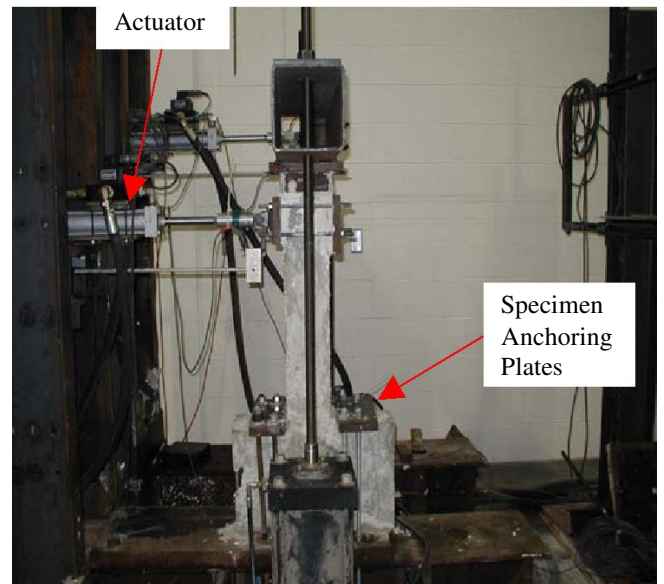
6.3.2 Fabrication

In order to secure the reinforced concrete test specimens to the existing actuator platform, the specimens were anchored to the platform such that no rotation or slip would occur between the column base and platform surface. To accomplish this, one-inch thick steel plates were placed onto the base of the columns and three-quarter inch threaded rods were used to anchor the column to the platform, as shown in Figures 6.5 and 6.6b. Ultracal 30 grout was used to ensure an even and level surface between the column and platform surface. The hydraulic actuator plates, used to provide a cyclic shear loading onto the column, were similarly grouted to the column specimens.

To minimize time needed to fabricate the experimental setup, two pneumatic jacks [shown in Figures 6.5 and 6.6a.] were utilized to provide a static gravity load of 30 kips to the specimens; the gravity/axial load supplied by the pneumatic jacks is representative of the inertial mass of the structure supported by each column specimen. The box beam [Figure 6.6a.], connected in tension to the pneumatic jacks, was supported by angle irons that capped the column and secured the beam on top of the column preventing slip between the column and beam; this connection also served to prevent out of plane motion of the column during testing. The pneumatic jacks were anchored to the ground by steel A36 gussets [Figure 6.6c.], dimensioned to withstand the buckling and shear loads developed within the gussets due to the upward force imposed by the pneumatic jacks, which were welded to the web of the wide-flange test platform. The pneumatic jacks were also positioned such that they would move in unison with the column and in the direction of the actuator motion (shear load).



a.



b.

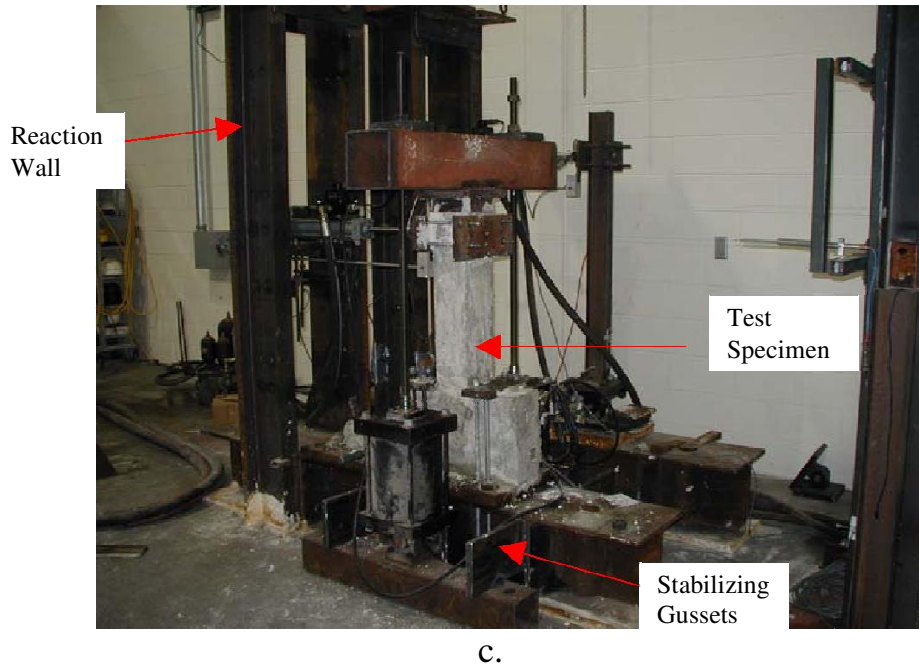


Figure 6.6: Fabrication of experimental setup for quasi-static tests on specimens. a. Side view of setup b. Front view of setup c. Overall experimental setup

Each pneumatic jack was calibrated to provide one-half of the total axial load that would be placed onto the column specimens on the gussets. Each column specimen was then moved to the earthquake simulator in the PEER lab at the Richmond Field Station before testing. Specimens were aligned with the intended shaking direction and bolted in place.

6.4 EXPERIMENTAL PROGRAM

Columns were fixed such that there was no moment between column ends while the column was subjected to a series of lateral displacements at increasing displacement amplitudes (i.e. $0.5\Delta_y$, Δ_y , $2\Delta_y$, etc.), where Δ_y is the column yield displacement, with three cycles at each displacement amplitude. The frequency of each cycle was 0.025 inch displacement per second up to yield displacement and 0.05 in. displacement per second for displacements after yield and up to the point of axial load failure. This frequency of shear loading was chosen because it would impose a cyclic motion of long enough duration (i.e. up to $4\Delta_y$ or 4 ductility) needed to reasonably observe damage progression in the columns up to axial failure, while also being of slow enough frequency to observe gradual shear degradation occurring with each specimen.

Since each column specimen was not tested as part of a larger reinforced concrete frame structure, no load redistribution after axial load failure in the column is possible. Thus, once axial load failure occurred in the test specimens, the quasi-static tests were terminated.

A calculated yield displacement, determined from Equation 2.4, was used to formulate the displacement steps used in the experimental program and compared to the perceived yield

displacement given by the hysteretic column response graph recorded by the Automated Test System (ATS), a test control and data acquisition system used to monitor and control the displacement of the hydraulic actuator; if the calculated yield displacement was found to differ from the perceived yield displacement, the experimental program was reassessed based on the perceived yield displacement.

Instrumentation used in the test program consisted of a displacement transducer connected to the length of the column and one connected to the base of the column. The transducer connected along the length of each column specimen was used to experimentally measure the horizontal displacement exhibited by the column throughout the test; the transducer attached to the column base, on the other hand, was used to measure any slip occurring between the column and platform.

The results of this experimental program for each test specimen are presented in Chapter 7 and analyzed in Chapter 8.

7 Quasi-Static Test Results

7.1 INTRODUCTION

This chapter presents the various damage states observed in each test specimen, as well as measured hysteretic response of the test specimens to dynamic shear and static gravity loading. The experimental results presented in this chapter are later compared in Chapter 8, to the results predicted by the capacity models introduced in Chapters 2, 4 and 5.

7.2 SHEAR-FAILURE TESTS

This section presents the actual displacement history and experimental program subjected onto test specimens 1 and 2, as modified during testing from the target displacement program introduced in Section 6.4. More importantly, this section introduces the force-deformation behavior or *hysteretic response* of both test specimens to bidirectional loading and compares these results with visual observations of damage progression made during the course of testing.

7.2.1 Specimen 1

Specimen 1 was subjected to the experimental test program shown in Table 7.1.

Table 7.1: Experimental test program conducted on specimen 1.

Yield Displacement, ΔY_{calc} (in) 0.213594 in				Axial Load, P 29.5 kips			
Ductility	+/- Displacement (in)	Total Stroke Length (in)	Cycle Period (sec)	Cycle Frequency (hz)	Test Velocity (in/sec)	# of Cycles	Observations during test
						0.5	Actuator start up
1.16 ΔY_{calc}	0.247	0.494	39.52	0.0253	0.025	3	
2.3 ΔY_{calc}	0.494	0.988	79.04	0.01265	0.025	3	Appears to yield at 0.3 in
2.8 ΔY_{calc}	0.6	1.2	96	0.01042	0.025	3	
4.62 ΔY_{calc}	0.987	1.974	78.96	0.01266	0.05	3	1 st half of 1 st cycle-shear failure, 1 st half of 2 nd cycle-axial failure

7.2.1.1. Progression of Observed Damage

Initially, at 1.16 yield displacement or 1.16 ductility, there was no visible elastic deformation. However, during the 3rd cycle at displacement step 1.16 yield, some initial, temporary cracking was detected after one complete cycle and observed to take place at the column-base joint of specimen 1 when the hydraulic actuator pushed, in tension, the specimen. No permanent cracks were observed in the test specimen at the end of the 3 cycles at 1.16 yield displacement.

At the beginning of the first cycle at 2.3 times yield displacement [2.3 ductility], yielding of the longitudinal reinforcement was determined to have occurred based on the hysteretic response of the test specimen as read from the ATS system, discussed in Section 6.4; yielding of the longitudinal reinforcement was defined from the ATS readings by the peak shear load sustained by the specimen as determined from by the hysteretic response curve. Two horizontal, permanent cracks were observed at the column-base joint at 2.3 ductility where the deep cracking resulting on one side of the column may be due to the position of the column anchoring plates and their restriction of lateral deflection at the base-column joint. Horizontal cracks were observed approximately 3 inches above the column base. Slight crushing of concrete then took place along the column-base joint with very little spalling of the concrete observed; the damage state of specimen 1 at first yielding of the longitudinal reinforcement is shown in Figure 7.1a.



a.



b.



c.



Figure 7.1: Progression of damage in specimen 1.

a. Damage state at yielding of longitudinal reinforcement. b. Shear failure. c. Axial load failure.

At 4.62 times yield displacement [4.62 ductility] and after the 1st half of the first cycle, a fine diagonal crack appeared indicating the formation of a shear failure plane in the test specimen, as evident in Figure 7.1b. The phenomenon of buckling of the longitudinal reinforcements is evident at this stage and can also be seen in Figure 7.1b. During the 2nd half of the first cycle at 4.62 ductility, extensive damage was initiated in the specimen with large blocks of concrete spalling off the column and opening of the crack along the shear failure plane observed. Due to the extensive buckling of the longitudinal reinforcements, further concrete spalling occurred due to severe crushing along the shear failure plane. During the 1st half of the second cycle at 4.62 ductility, total collapse (i.e. axial load failure) of the specimen resulted; the damage state at axial load failure for specimen 1 can be seen from Figures 7.1c. and 7.2.

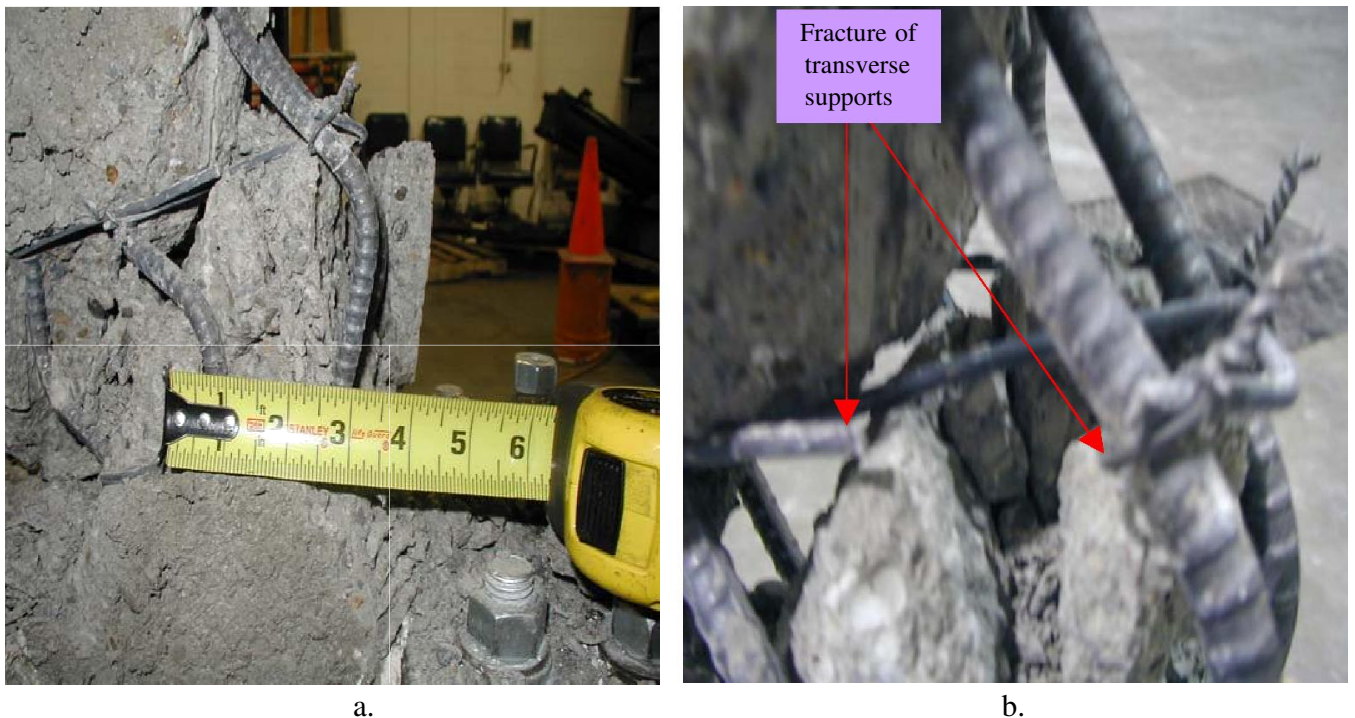


Figure 7.2: Specimen 1 damage at axial load failure.

a. Buckling of longitudinal reinforcement. b. Fracture of transverse reinforcement.

The damage state of specimen 1 at axial load failure can be observed from Figure 7.2 by the fracture of the transverse reinforcement and resulting, maximum longitudinal reinforcement buckling of 3 in.

7.2.1.2 Measured Response

This section presents the hysteretic response of specimen 1 recorded during experimentation. The displacement history subjected onto specimen 1 is shown in Figure 7.3 and was based on the experimental program described in Section 6.4.

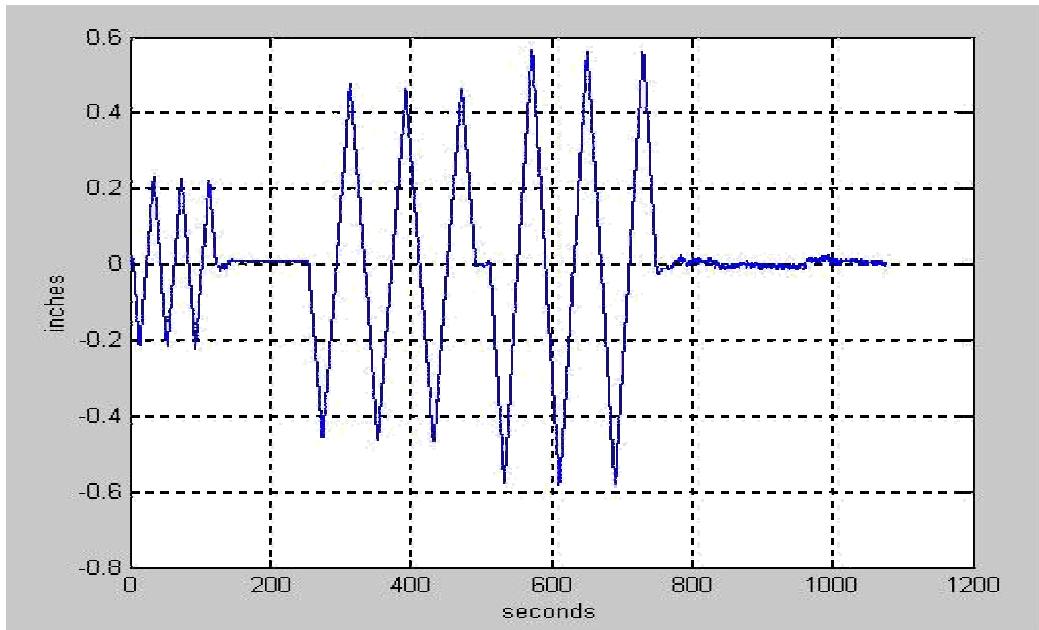


Figure 7.3: Modified target displacement history for specimen 1.

The force-deformation response of specimen 1 is shown in Figure 7.4.

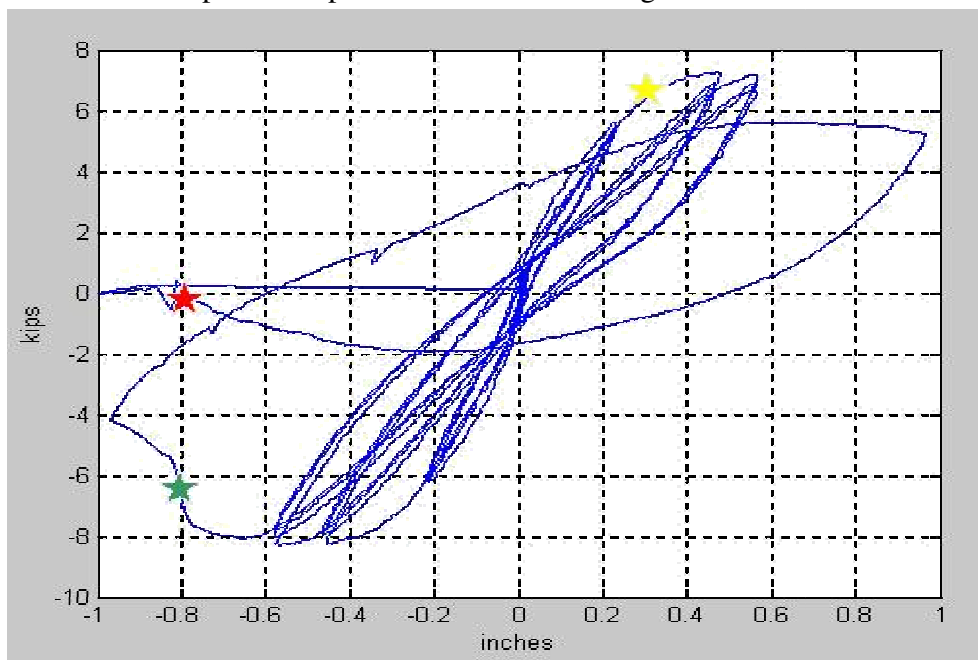


Figure 7.4: Experimental force-displacement response of specimen 1

First yielding of the longitudinal reinforcement in specimen 1 is observed to occur at 0.3 inches lateral displacement and is indicated on Figure 7.4 by a yellow marker. The damage state for the specimen at yielding is shown in Figure 7.1a.

The occurrence of shear failure in specimen 1 is indicated by the green marker in Figure 7.4. Shear failure is defined, in this report, by a 20 percent drop in shear load carried by the specimen as observed on the hysteretic response curve. At the beginning of cyclic loading at a ductility of 4.62, the peak shear load sustained by the specimen prior to the initiation of shear failure is 8.2 kips; thus, a 20 percent drop in shear load (i.e. shear failure) occurs during the 1st half of the first cycle under a shear load of approximately 6.56 kips. This loss of shear load capacity corresponds with the pronounced crack developed within the specimen along a shear failure plane, shown in Figure 7.1b. After shear failure, specimen 1 undergoes further shear capacity degradation prior to axial load failure.

Since the onset of axial load failure in a shear-critical reinforced concrete column is defined by a complete loss of shear load capacity, axial load failure in specimen 1 is indicated in Figure 7.4 by the point on the hysteretic curve where zero shear load is sustained by the specimen. Axial load failure is indicated on Figure 7.4 by the red marker and occurs 1 cycle after shear failure. The occurrence of axial load failure in specimen 1 concurs with the damage progression observed in the specimen as shown in Figures 7.1c. and 7.2.

7.2. Specimen 2

Specimen 2 was subjected to the experimental test program shown in Table 7.2.

Table 7.2: Experimental test program conducted on specimen 2.

Yield Displacement, ΔY_{calc} (in) 0.213594 in				Axial Load, P 29.5 kips			
Ductility	+/- Displacement (in)	Total Stroke Length (in)	Cycle Period (sec)	Cycle Frequency (hz)	Test Velocity (in/sec)	# of Cycles	Observations during test
						0.5	Actuator start up
0.75 ΔY_{calc}	0.16	0.32	25.6	0.03906	0.025	3	
1.5 ΔY_{calc}	0.32	0.64	51.2	0.01953	0.025	3	Appears to yield at 0.3 in
3 ΔY_{calc}	0.64	1.28	102.4	0.00977	0.025	3	
4.5 ΔY_{calc}	0.96	1.92	76.8	0.01302	0.05	3	1 st half of 1 st cycle-shear failure, 1 st half of 2 nd cycle-axial failure

7.2.2.1. Progression of Observed Damage

No noticeable yielding or cracking occurred with cycling at 0.75 ductility. In the 1st half of the 2nd cycle at 1.5 ductility, yielding of the longitudinal reinforcement was also determined to have occurred based on the hysteretic response of the test specimen as read from the ATS system, discussed in Section 6.4. Between the 3rd cycle at 1.5 ductility and 2nd cycle at 3 ductility, slight horizontal cracks became evident at the column-base joint; however, the horizontal cracks and concrete spalling occurring in specimen 2 at yielding were not as visibly noticeable as those occurring in specimen 1; thus, pictures of specimen 1 yielding were omitted from this report.

In the 1st half of the 1st cycle at 3 ductility, a fine diagonal crack appeared on the specimen indicating development of a shear failure plane in the specimen; further definition of the shear failure plane, as well as severe outward buckling of longitudinal reinforcement took place throughout displacement cycles at 3 ductility, indicating a failure of the transverse reinforcement at approximately 4 inches above the column base [Figure 7.5b.]. As a result, a large section of concrete began to spall off on one side of the specimen column, as can be seen from Figure 7.5a.

During the 2nd half of the first cycle at 4.5 ductility, extensive damage was initiated in the specimen with a large intact block of concrete buckling outward along one side of the column, some localized concrete spalling, and opening of the crack along the shear failure plane observed. During the 1st half of the second cycle at 4.5 ductility, axial load failure occurred in the specimen as observed by the complete loss of concrete cover above the column- base joint and crushing along the shear failure plane. The final damage state of specimen 2 at axial load failure is shown in Figure 7.6. The specimen slid along failure plane due to the gravity loads

remaining and thus, exposing the buckling of the longitudinal reinforcements and fracture of the transverse supports. Total collapse (i.e. axial load failure) of the specimen resulted; the damage state at axial load failure for specimen 2 is seen in Figure 7.6.



a.



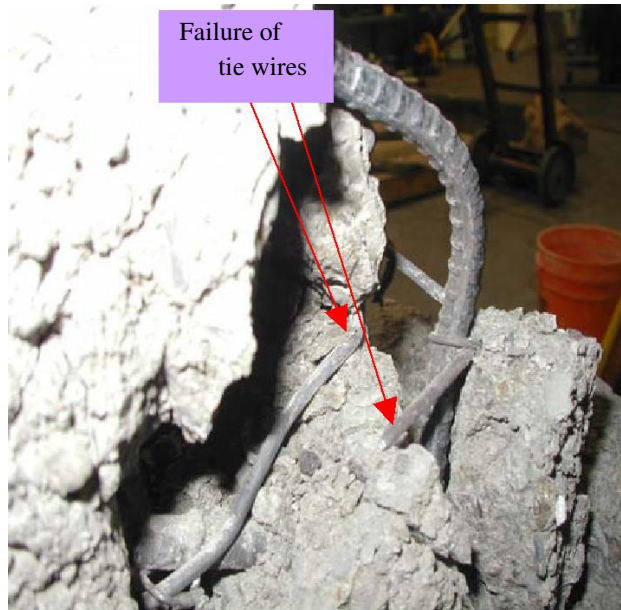
b.



Figure 7.5: Progression of damage in specimen 2.

a. Shear failure. b. Axial load failure.

Similar to the case of specimen 1, the damage state of specimen 2 at axial load failure can be observed from Figure 7.6b. by the maximum longitudinal reinforcement buckling of 3 in. occurring approximately 5.5 inches above the column-base joint. However, unlike specimen 1, failure of the transverse reinforcements to contain the concrete core and longitudinal reinforcement did not occur due to fracture of the transverse supports; rather, failure in the tie wires used to bind the free ends of the transverse reinforcement were at fault [Figure 7.6a.].



a.



b.

Figure 7.6: Specimen 2 damage at axial load failure.

a. Fracture of transverse reinforcement. b. Buckling of longitudinal reinforcement.

7.2.2.2 Measured Response

This section presents the hysteretic response of specimen 2 recorded during experimentation. The displacement history subjected onto specimen 2 is shown in Figure 7.7 and was based on the experimental program described in Section 6.4.

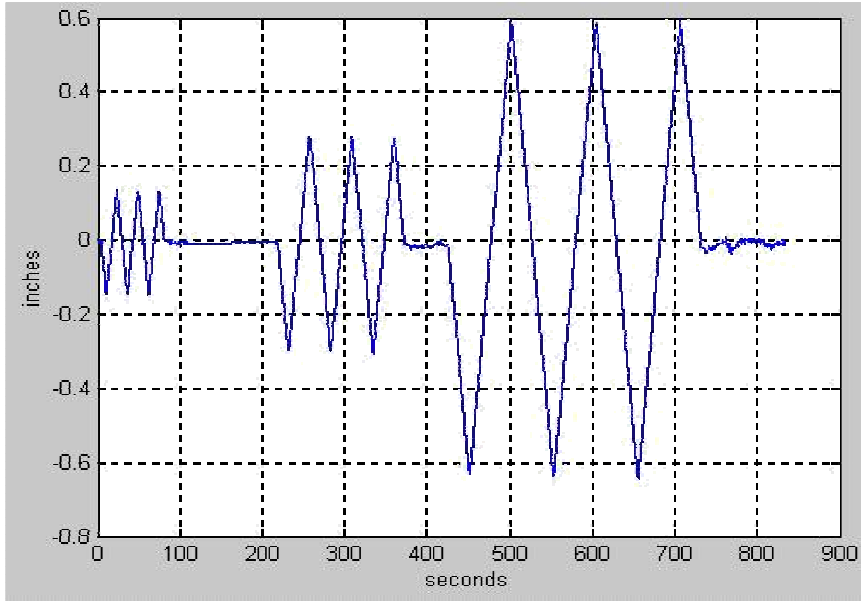


Figure 7.7: Modified target displacement history for specimen 2.

Figure 7.8 shows the shear hysteretic response of specimen 2.

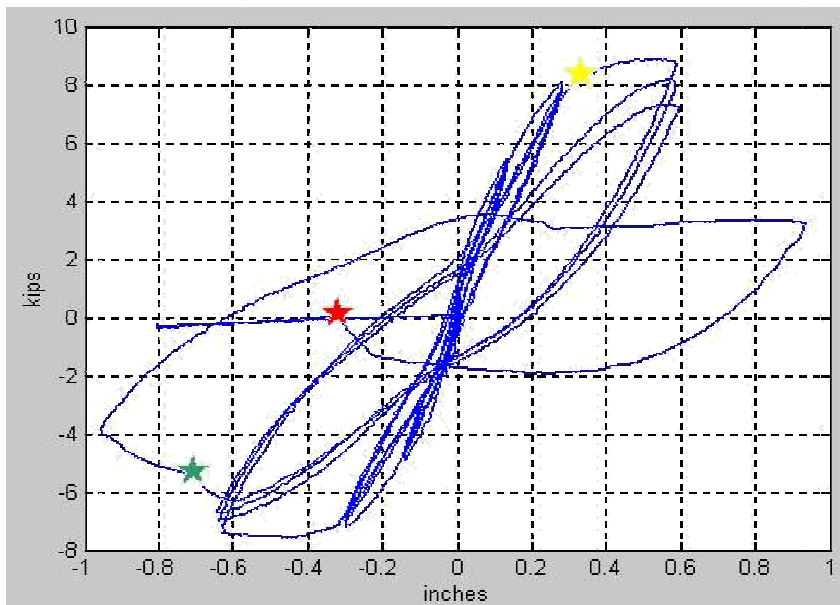


Figure 7.8: Experimental force-displacement response of specimen 2

As for the hysteretic response for specimen 1, the damage states for specimen 2 are indicated by the colored markers in Figure 7.8: first yielding of the longitudinal reinforcement is represented by a yellow marker, shear failure by a green marker and axial load failure by a red marker.

For specimen 2, yielding was also observed to have occurred at approximately 0.3 inches lateral displacement

Prior to cyclic loading at a ductility of 4.5, the peak shear load sustained by the specimen is approximately 6.2 kips; thus, a 20 percent drop in shear load and initiation of shear failure in the specimen occurs during the 1st half of the first cycle under a shear load of approximately 5 kips. This drop in shear load coincides with the development of severe cracking along the shear failure plane and is accompanied by the continued crushing of concrete at the column-base joint, as evident in Figure 7.5a. After shear failure, it can be seen from the hysteretic response curve that specimen 2 undergoes a significant degradation of shear load capacity between the 1st half of the first cycle and the 1st half of the second cycle.

Since the onset of axial load failure is defined to have occurred when the specimen has zero shear-carrying capacity, axial load failure in specimen 2 was determined from Figure 7.8 to have occurred at a horizontal displacement of approximately 0.32 inches during the 1st half of the second cycle at 4.5 ductility, or one cycle after the occurrence of shear failure. The occurrence of axial failure in Figure 7.8 agrees with the observations of damage progression made during

this time and the total structural collapse along the shear failure plane took place which resulted; the damage states for the specimen at axial load failure are shown in Figures 7.5b. and 7.6.

9 Conclusion

Earthquake reconnaissance has shown that columns in reinforced concrete buildings constructed prior to the introduction of modern seismic ACI code in the early 1970s are particularly vulnerable to shear failure. The goal of this project was to develop validation data to test empirical capacity models which seek to predict the inelastic response and in particular, failure mechanisms of existing, shear-critical reinforced concrete columns to gravity and seismic loading. Quasi-static earthquake simulation tests on scaled shear-critical reinforced concrete columns were conducted and compared to the theoretical capacity models used to develop the PEER/UC Berkeley-developed *OpenSees* analytical program. As previously discussed, the RC structure deformation components and capacity models implemented in *OpenSees* had significant errors in predicting the hysteretic response of the shear-critical RC column test specimens under bi-directional loading. However, it is to be concluded that hysteretic data produced in this research cannot, by itself, either validate or invalidate the empirical capacity models used to develop *OpenSees* since the scaling methodology used to design and fabricate a scaled model of a shear-critical RC column from its prototype failed to produce hysteretic response data representative of the prototype column. Assumptions made in the scaling process oversimplified the design of the test specimens and thus, affected the integrity of the hysteretic data recorded. In other words, it is concluded that the validation data presented in this research does not accurately represent the actual inelastic behavior of full-size, shear-critical RC columns under unidirectional seismic loading.

Nevertheless, there is a need for further calibration of the *OpenSees* analytical model before such earthquake simulation models, at the expense of laboratory and field testing, are the sole influence factor in RC column seismic design and retrofit. Therefore, it is proposed that future research incorporating better scaling procedures be used to conduct cost-effective laboratory tests on scaled column models or large-scale column testing be undertaken for the purpose of producing validation data from which to calibrate developing analytical models. With appropriate calibration and further validation studies, a revised *OpenSees* program can be used to predict hysteretic response of existing shear-critical, RC beam-column frames under seismic & gravity loading. Further, based on individual RC column component validation tests, *OpenSees* would make it possible to predict the deformation response of existing, multistory RC building frames subjected to gravity load and various MDOF seismic loading pattern...